

# The effect of social groups on the dynamics of bi-directional pedestrian flow: a numerical study

Francesco Zanlungo<sup>\*1</sup>, Luca Crociani<sup>2</sup>, Zeynep Yücel<sup>1,3</sup> and Takayuki Kanda<sup>1,4</sup>

<sup>1</sup>ATR International, Kyoto, Japan

<sup>2</sup>Bicocca University, Milan, Italy

<sup>3</sup>Okayama University, Okayama, Japan

<sup>4</sup>Kyoto University, Kyoto, Japan

June 30, 2021

## Abstract

*Pedestrian social groups represent a large portion of urban crowds and are expected to have a considerable effect on their dynamics. In this work we investigate the effect of groups on a bi-directional flow, by using novel computational methods. Our focus is on self-organisation phenomena, and more specifically on the time needed for the occurrence of pedestrian lanes, their stability and their effect on the velocity-density relation. Moreover, we are interested in understanding the amount of physical contact in the crowd. To this end, we use a novel model considering the asymmetrical shape of the human body and describing its rotation during collision avoidance, and combine it to previously published mathematical model of group behaviour, based on real world uncontrolled observations of pedestrians in low to moderate densities. We configure several scenarios by varying the global density  $\rho$  of pedestrians and the ratio  $r_g$  describing the percentage of grouped pedestrians in the simulation. Our results show that the presence of groups has a significant effect on velocity and lane organisation, and a dramatic one on collision. Specifically, crowds with groups walk with slower velocity (excluding at very high densities), need more time to organise in lanes and have less pedestrians in lanes; the number of lanes is also significantly different, at least for some value of  $\rho$ . As stated, the most dramatic effect is on collisions, which are increased of an order of magnitude in presence of groups. We are well aware of the limitations of our approach, in particular concerning (i) the lack of calibration of body rotation in collision avoidance on actual data and (ii) straightforward application of a low density group model to higher density settings. We nevertheless want to stress that it is not our intention to state that our results reproduce the actual effect of groups on bi-directional flow. In particular, it seems highly unrealistic that crowds with groups collide extremely more often. Nevertheless we believe that our results show the great theoretical and practical implication of the consideration of realistic group behaviour in pedestrian models, and suggest that realistic results may hardly be achieved simply by adding together modular models.*

---

<sup>\*</sup>zanlungo@atr.jp

# 1 Introduction

Pedestrian physical crowds, i.e. not sharing a social identity [1], are nevertheless characterised by the presence of a large number of social groups [2]. As a result, it has to be expected that the presence of such groups, i.e. of pedestrians that move together and with peculiar velocity pattern and spatial formation [3, 4], may strongly influence the dynamics of the crowd [5]. Although a few microscopic models of group have been recently introduced, [2, 3, 6, 7, 8, 9, 10, 13, 14, 15, 16, 17, 18, 19, 20, 21, 22, 23, 24, 25, 26, 27], a quantitative assessing of the effect of groups on crowd dynamics is still far from being achieved. This is also due to the fact that, related to the lack of quantitative empirical data, we are still lacking realistic models of how groups behave *at different density ranges* (not to mention how they behave under different conditions e.g. commuting vs shopping vs evacuation; [28, 29] show that purpose, relation, gender, age and height all have a strong impact on group dynamics).

The purpose of this work is not to provide a definitive answer to these problems, but to show and investigate their relevance. To this end, we are going to

- use a realistic mathematical model for the behaviour of pedestrian groups in low to moderate density settings,
- combine it to a realistic and efficient collision avoidance model
- and use the resulting model to investigate the effect of the presence of groups on self-organisation properties of a bi-directional flow (velocity/fundamental diagram, amount of collisions, number of lanes and rate of pedestrians moving in lanes; these quantities being analysed both in their transition and equilibrium).

## 2 Group behaviour

In [3], we introduced a mathematical model, based on a pair-wise interaction potential, describing the dynamics of socially interacting pedestrian groups. Writing the relative position between two socially interacting pedestrians  $i$  and  $j$  as  $\mathbf{r}_{ij} \equiv \mathbf{r}_i - \mathbf{r}_j = (r_{ij}, \theta_{ij})$ , where  $\theta = 0$  gives the direction to the pedestrians' goal, the discomfort of  $i$  due to not being located in the optimal position for social interaction with  $j$  is given by the (discomfort) *potential*<sup>1</sup>

$$\begin{aligned}
 U^\eta(r_{ij}, \theta_{ij}) &= R(r_{ij}) + \Theta^\eta(\theta_{ij}), \\
 R(r) &= C_r \left( \frac{r}{r_0} + \frac{r_0}{r} \right), \\
 \Theta^\eta(\theta) &= C_\theta \left( (1 + \eta)\theta^2 + (1 - \eta)(\theta - \text{sign}(\theta)\pi)^2 \right),
 \end{aligned} \tag{1}$$

---

<sup>1</sup>In Eq. 1, we are assuming  $-\pi < \theta < \pi$ , and using  $\text{sign}(0) = -1$  in order to have a continuous potential. Refer to the original work for details.

where  $r_0$  is the most comfortable interaction distance, and  $-1 \leq \eta < 0$  is related to the intensity of social interaction. The acceleration of the pedestrian  $i$  due to group dynamics, i.e. the action of the pedestrian aimed to minimise social interaction discomfort with respect to  $j$ , is given by

$$\mathbf{F}_{ij}^{first} = -\nabla_i U^\eta(\mathbf{r}_{ij}). \quad (2)$$

In the potential of Eq. 1, the radial term  $R$  assures that the pedestrians will have a distance close to  $r_0$ , while the angular potential  $\Theta^\eta$  allows them to keep both their interaction partner and their walking goal in sight (the more negative  $\eta$  is, the more pedestrians will try to have interaction partners in their vision field). In a pedestrian group, first neighbours interact through the force of Eq. 2, while second neighbours interact through a weaker and simplified potential depending only on the radial potential of Eq. 3 [30],

$$\mathbf{F}_{ij}^{second} = -\frac{1}{2}\nabla_i R(r_{ij}). \quad (3)$$

In this model, a pedestrian's neighbourhood is decided based on its position on the axis orthogonal to the direction of the goal, see [30] for details.

From the model, under the assumption that in large, low density settings, the combined effect of external influence, individual variation and "randomness" in the decision process may be modelled through white Gaussian noise, it is possible to derive a Langevin equation for the motion of pedestrians and a Boltzmann distribution for the pdf of pedestrian position in a two people group. Such a distribution was used to calibrate the model by comparing with actual data collected in a pedestrian facility under conditions in agreement with the models' assumptions.

The model, in agreement with observational data, predicts that 2 people groups:

- *are slower than individual pedestrians*, and in particular the velocity of the group is given by

$$v^2 \approx v^p + \frac{2C_\theta\eta\pi}{r_0\kappa} < v^p, \quad (4)$$

where  $v^p$  is the individual preferred velocity,

- *walk in an abreast formation*, the pdf for positions in centre of mass of the group following a *bean shaped distribution*,

while 3 people groups:

- are even slower, with

$$v^3 \approx v^p + \frac{8C_\theta\eta\pi}{3r_0\kappa} < v^2, \quad (5)$$

- *walk in a V formation*, with the central pedestrian behind and the two pedestrians on the wings slightly ahead.

### 3 Collision avoidance

#### 3.1 Long range (circular)

[31] shows that the group model of [3, 30] may be effectively combined with a collision avoidance module. More specifically, the model used in [31] was derived by [32]. The basic idea of such model is the following: for all pedestrians we compute, with respect to every obstacle  $i$  in their neighbourhood (including moving ones, such as other pedestrians), the time  $t_i$  at which they will reach the minimum distance to such obstacle, assuming both the pedestrian and the obstacle will keep a constant velocity. We then define

$$t_{min} = \min_{i, t_i > 0} t_i, \quad (6)$$

and, again assuming linear motion at constant velocity,

$$\mathbf{r}_i^{min} = \mathbf{r}_i(t_{min}) - \mathbf{r}(t_{min}), \quad (7)$$

i.e., the difference between the position of the obstacle  $\mathbf{r}_i$  and the of the pedestrian  $\mathbf{r}$  at  $t_{min}$ .

Such “future distance”  $\mathbf{r}_i^{min}$  is then used to define a the collision avoidance term of a velocity dependent specification of the social force model [33] as

$$\mathbf{F}_i = \frac{v}{t_{min}} \mathbf{F}(\mathbf{r}_i^{min}) \quad (8)$$

$v$  being the magnitude of the pedestrian’s velocity. While in [32], for historical reasons, the choice of  $\mathbf{F}$  resembled the one of [33], just replacing current with future positions, following the analysis of [34] in [31] and in the current work we use hard core potentials

$$\mathbf{F}(\mathbf{r}) = \begin{cases} A & \text{if } r \leq d_1, \\ A \frac{d_2 - r}{d_2 - d_1} & \text{if } d_1 < r \leq d_2, \\ 0 & \text{if } r > d_2. \end{cases} \quad (9)$$

#### 3.2 Short range (ellipse)

We recall that according to the Social Force Model paradigm, the pedestrian decision process determines their acceleration as

$$\ddot{\mathbf{r}} = -k_1(\dot{\mathbf{r}} - \mathbf{v}_p) + \mathbf{F}_{int}. \quad (10)$$

Here  $\mathbf{v}_p$  is the preferred velocity of the pedestrians, while  $\mathbf{F}_{int}$  is the interaction (social) force<sup>2</sup>. In the model of [32] this term is given by the sum of over all obstacles  $i$  in eq. 8.

The model of [32] was designed for moderate densities and did not take in account the shape of the human body. In order to describe the motion of pedestrians at high density is necessary to consider at least the fact that the 2D projection of the human body is

---

<sup>2</sup>Usually when dealing with social forces masses are set to 1.

not symmetrical (this asymmetry may be first approximated by using ellipses instead of circles). When such an asymmetry is introduced, even if we still limit ourselves to the motion of pedestrians on a 2D plane, we need to introduce a new degree of freedom, body orientation angle  $\theta$ . Assuming body orientation to be equal to velocity orientation would be a too strong limitation, since it would not allow pedestrians to rotate their torso while avoiding a collision without changing considerably their motion direction. We thus consider the pedestrian to be characterised by 3 degrees of freedom, 2D position  $\mathbf{r} = (x, y)$  and angle  $\theta$ . The latter variable identifies the orientation of an ellipse with axes  $(A, B)$  (45 and 20 cms).

As we are operating in the Social Force Model paradigm, we deal with second order differential equations for the pedestrian linear and angular acceleration  $\ddot{\mathbf{r}}$  and  $\ddot{\theta}$ , as functions of  $\mathbf{r}$ ,  $\dot{\mathbf{r}}$ ,  $\theta$  and  $\dot{\theta}$ . Assuming the  $\mathbf{r}$  and  $\theta$  equations to be decoupled is highly unrealistic, since, while pedestrians are indeed able to walk in a direction different from their body orientation, they prefer moving in the direction of their body orientation. By ignoring for the moment body oscillations due to gait, we propose the following equations

$$\ddot{\mathbf{r}} = -k_1(\dot{\mathbf{r}} - \mathbf{v}_p) - k_2\Phi(\dot{\mathbf{r}}, \theta) + (1 - \beta(t_c))\mathbf{F}^C + \beta(t_c)\mathbf{F}^E + \mathbf{F}^G, \quad (11)$$

and

$$\ddot{\theta} = -k_3\dot{\theta} - k_4\Phi(\dot{\mathbf{r}}, \theta) + \beta(t_c)T^E. \quad (12)$$

Many terms deserve to be explained. By  $\mathbf{F}^G$  we denote the forces determined by the group potential of [30]<sup>3</sup>, and by  $\mathbf{F}^C$  the “circular” collision avoidance forces of [32]<sup>4</sup>.  $k_2$ ,  $k_3$  and  $k_4$  are model parameter.  $k_3$  accounts for the tendency of reducing body oscillations, while  $k_2$  and  $k_4$  for the tendency of walking in the direction of body orientation, through the angle difference between velocity and body orientation given by  $\Phi$ .  $t_c$  is the time at which the first collision will happen between the ellipse representing the pedestrian body and an obstacle (such as a wall or another pedestrian), computed using an event driven algorithm [35] under the assumption of no acceleration. The function  $\beta$  introduces the idea that far away collisions are managed just using the model of [32], while close ones use forces taking in account body shape ( $\mathbf{F}^E$ , defined below). In detail,  $\beta$  introduces two time scales  $\tau_1$ ,  $\tau_2$  such that

$$\beta(t) = \begin{cases} 1 & \text{if } t \leq \tau_1, \\ \frac{\tau_2 - t}{\tau_2 - \tau_1} & \text{if } \tau_1 < t \leq \tau_2, \\ 0 & \text{if } t > \tau_2. \end{cases} \quad (13)$$

As stated above, we use an event driven algorithm to compute the time of the next collision between ellipses and obstacles (polygons or other ellipses). This algorithm can be used to reproduce the dynamics of hard ellipses undergoing elastic collisions, i.e., it provides also the force and torque that the ellipse undergoes at the moment of collision, under the assumption of impenetrability and conservation of energy and momentum<sup>5</sup>.

<sup>3</sup>Whose dependence on the group member positions is not shown for reasons of simplicity of notation.

<sup>4</sup>Again dependent of positions and velocities of the pedestrian and of all obstacles.

<sup>5</sup>These are actually impulsive forces and torques, i.e., expressed as a instantaneous change in linear and angular momentum.

These forces and momentum can be used as the basis of a collision avoidance method. Let us for simplicity consider the case of a 2D disc (i.e. ignoring  $\theta$ ) colliding frontally with a wall at velocity  $\mathbf{v}$  in time  $t$  ( $t$  is the time from now at which the collision will happen if the pedestrian velocity is not modified). At the moment of collision, the pedestrian will undergo a change in velocity  $\Delta\mathbf{v} = -2\mathbf{v}$ . If a force  $\Delta\mathbf{v}/2t$  is applied on the pedestrian, collision will be avoided, with the pedestrian just stopping short of the collision. By generalising to the elliptical case, we define

$$\mathbf{F}^E = \frac{\gamma}{t_c} \Delta\mathbf{p} \quad (14)$$

$$\mathbf{T}^E = \frac{\gamma}{t_c} \Delta\mathbf{L} \quad (15)$$

here  $\gamma$  is a model parameter, and  $\Delta\mathbf{p}$  and  $\Delta\mathbf{L}$  are, respectively, the linear and angular momentum exchanged at the time of collision.

Equations 11 and 12 realise the “social” interaction of pedestrians, i.e. their decisional process, that is, for simplicity’s sake, realised at a fixed time step  $\Delta t = 0.05$  s (i.e., the decisional dynamics is solved by using an Euler integrator). For the physical dynamics of the system, i.e. in order to deal with *actual* (as opposed to predicted) collisions between pedestrians, we use again an event driven algorithm for elastic collisions between ellipses. Such an algorithm has the positive properties to force absence of overlapping, and thus constraints on space occupation, and to provide a quantitative measure for the amount of collisions (kinetic energy, both linear and angular, exchanged in collisions). The negative aspect is that elastic collisions are not very realistic between pedestrians, but this problem should not be a serious one for a functional collision avoidance method, i.e. a method in which collisions are extremely reduced.

### 3.3 Optimisation

The parameters concerning group behaviour are taken directly from [3, 30]. As stated above, the purpose of this paper is to investigate what are the possible issues of combining a collision avoidance model with a group behaviour model, and due to the absence of data concerning both body rotation in collision avoidance and group behaviour in uncontrolled high density settings, we decided to try first to develop an efficient collision avoidance model although not necessarily a realistic one.

We decided to use a genetic algorithm to fix the remaining parameters of the model according to the following approach. A given solution (set of model parameters) was tested on a mixed population of individual pedestrians and pedestrians in groups (of 2 or 3 members), moving in a bi-directional flow inside a corridor with an average density of 1 pedestrian per square meter. Using periodic boundary conditions and a fixed simulation time, for each solution we computed the following quantities<sup>6</sup>:

- Amount of energy exchanged in collisions  $E$ ,
- Difference between moving direction and body orientation  $|\Phi|$ ,

---

<sup>6</sup>Averaged over all pedestrians and simulation time.

- Difference between preferred velocity and actual velocity  $|\delta v|$ ,
- Number of pedestrians  $n$  falling at a close distance  $d < 0.6$  m,
- Group potential  $P$  from [3] (the higher the value, the more pedestrians are far from their preferred group configuration).

It is reasonable that pedestrian may want to minimise all the above quantities, so that a possible candidate for a fitness function is

$$f = -(w_E E + w_\Phi |\Phi| + w_\delta |\delta v| + w_n n + w_P P), \quad (16)$$

Nevertheless it is not trivial to decide the values of the weights, considering also that different dimensions of the terms. The chosen solution was to define the weights in the following way. For example, we define

$$w_E = \frac{1}{E_{min}} \quad (17)$$

where  $E_{min}$  is the optimal value of  $E$  obtained by using a fitness function with the only term  $f = -E$ . By proceeding in a similar way for all weights, we finally obtained an adimensional fitness function that we used to optimise our model parameters.

## 4 Experiments

### 4.1 Experimental setting

In our simulations we use a corridor of width 3 meters and length 20 meters, and periodic boundary conditions. The width of the corridor is chosen in such a way that two 3 people groups walking in opposite directions may not cross without changing their formation, based on the group spatial size as reported in [3]. We use four different density conditions,  $\rho = 1$  ped/m<sup>2</sup>, i.e. 60 pedestrians,  $\rho = 2$  ped/m<sup>2</sup>, i.e. (120 pedestrians),  $\rho = 3$  ped/m<sup>2</sup>, (180 pedestrians) and  $\rho = 4$  ped/m<sup>2</sup> (240 pedestrians). We also use two different group rate  $r_g$  conditions, namely without groups  $r_g = 0$  and with half of the pedestrians in groups,  $r_g = 0.5$ . When groups are present, 20% of them are in 3 people groups, and 30% of them in 2 people groups. We thus have 8 conditions depending on the values of  $\rho$  and  $r_g$ . For example, when  $\rho = 4$  ped/m<sup>2</sup> and  $r_g = 0.5$  we have 120 individual pedestrians, 36 2 people groups and 16 3 people groups. Initial conditions are determined by dividing the corridor in cells of equal size, and placing pedestrians in randomly chosen cells, regardless of their flow direction<sup>7</sup>. The pedestrians' preferred velocities are chosen from a normal distribution with  $\mu = 1.2$  m/s and  $\sigma = 0.2$  m/s<sup>8</sup>. Each group or pedestrian has a probability 0.5 of belonging to each one of the flows<sup>9</sup>. For each condition, 10 different simulations with independent initial conditions are used and the observables defined below are averaged over these initial conditions.

<sup>7</sup>Pedestrians in the same group are nevertheless located in neighbouring cells.

<sup>8</sup>Pedestrians in the same group have the same preferred velocity.

<sup>9</sup>Thus flows have the same weight only in average.

## 4.2 Observables

For each experimental condition, we define the following observables:

- rate of velocity over preferred velocity,

$$\nu = \frac{v}{v_p} \quad (18)$$

- energy exchanged in collisions  $E$ ,
- number of lanes  $n_l$ ,
- rate of pedestrians in lanes

$$r_l = \frac{\sum_{i \in n_l} s_i}{N}, \quad (19)$$

where  $s_i$  is the number of pedestrians in lane  $i$  and  $N$  is the overall number of pedestrians.

Lane recognition is performed using the algorithm described below.

For each observable we first compute the average over pedestrians and time for each independent initial condition, and then compute the average, standard deviation and standard error over the different independent conditions. The latter are the values shown in the figures. In order to show also time dependence, time averages are computed over 10 slots of length  $T_i = 20$  s.

## 4.3 Lane clustering algorithm

For the analysis of the lane formation phenomenon we have applied the algorithm discussed in [11]. As a novel part of this paper, we have introduced an extended version of the algorithm which is able to produce more stable results in dense and possibly chaotic situations.

The algorithm is based on a hierarchical two-steps application of DBSCAN [12], with distance metrics and respective parameters specifically tailored to deal with this problem. The aim is to achieve clusters in tune with the intuitive conception of the lane formation phenomenon. The workflow is described in Fig. 1.

The choice of a hierarchical approach is mainly motivated by the need of knowing the average flow direction before the final identification of lanes: this information is in fact used to identify clusters which describe queuing pedestrians in the observed scenario. Moreover, we assume that the parameter *minPoints* –describing the smallest size of a cluster in DBSCAN– is set to 3 in both steps, since we define three persons walking in a river-like pattern as the simplest case of lane. The algorithm works on almost instantaneous data, potentially allowing the implementation on real-time systems: with the usage of a de-noising algorithm, smoothed positions and velocity vectors of pedestrians related to small time-windows ( $< 0.5$ s) can be calculated (in this work we did not use particular smoothing methods since the outcome positions from the simulation model are already sufficiently clean).



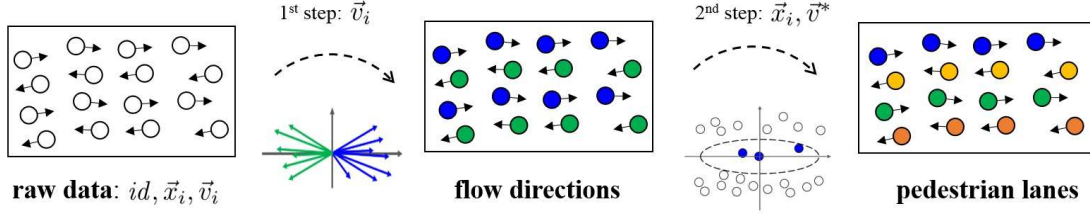


Figure 1: Workflow of the hierarchical clustering algorithm to characterize the lane formation.

The two steps of the algorithm are defined to compute clusters describing respectively: (i) the dominant flow directions in the observed scenario; (ii) the actual lanes of pedestrians. The dominant flow directions are achieved by aggregating velocity vectors  $\vec{v}_i$  of pedestrians, using the cosin dissimilarity as distance metric. This metric describes the angle  $\alpha_{ij}$  between two velocity vectors:

$$\alpha_{ij} = \arccos \left( \frac{\vec{v}_i \cdot \vec{v}_j}{\|\vec{v}_i\| \cdot \|\vec{v}_j\|} \right) \quad (20)$$

Two vectors  $\vec{v}_i$  and  $\vec{v}_j$  are considered *neighbours* if  $\alpha_{ij} \leq \Theta_\nu$ . Following the logic of DBSCAN, a point is then marked as *core* if it has at least *minPoints* neighbours, as *border* if it is neighbour of a core point or *noise* otherwise. A cluster is finally the set of all neighbour core and border points.

The output clusters of this first step are *dense* set of vectors, which should be representative of a direction of motion. This is verified in most of the cases, but it can happen that in particularly chaotic scenarios, where the observed crowd of pedestrian shows many patterns of movement directions, the whole set of vectors gets aggregated in a unique cluster. The output in this case is not representative of any direction of movement.

The problem can be overcome by acting on the parameters  $\Theta_\nu$  and *minPoints*. These two define the value of density searched in the dataset, thus it is possible to find a combination of parameters that leads to a proper segmentation of vectors among representative clusters. Acting statically on parameters is, though, a double-sided weapon: one might find a configuration which works perfectly with very dense and chaotic scenarios, but lacks proper results in more simple situations.

With these considerations, we configured an extension that iteratively adjusts the parameter *minPoints* for the current step analysed with the algorithm<sup>10</sup>, to further split clusters that do not satisfy a correctness criterion. The new version is described in Alg. 1, assuming *Points* to be the set of all velocities at the beginning of each frame and *max\_it* being the maximum number of iterations allowed to refine the result.

In this way, for a maximum of *max\_it* iterations, the algorithm will search for denser

<sup>10</sup>Note that at the beginning of each frame analysed with the algorithm, *minPoints* is reset to its initial value of 3.

---

**Algorithm 1** Iterative refining of velocity clusters.

---

```

1: while Points  $\neq \emptyset$  and max_it  $> 0$  do
2:   Vel_clusters  $\leftarrow$  compute_vel_clusters(Points,  $\Theta_\nu$ , minPoints)
3:   Points  $\leftarrow \emptyset$ 
4:   for Cluster  $\in$  Vel_clusters do
5:     if is_representative(Cluster) then
6:       Results  $\leftarrow$  Results  $\cup$  {Cluster}
7:     else
8:       Points  $\leftarrow$  Points  $\cup$  Cluster
9:     end if
10:  end for
11:  minPoints  $\leftarrow$  minPoints +  $\Delta_{points}$ 
12:  max_it  $\leftarrow$  max_it - 1
13: end while
14: return Results

```

---

clusters in the dataset until all achieved clusters do satisfy the *is\_representative* criterion. The increase of density among iterations is regulated via the  $\Delta_{points}$  parameter. Moreover, points in clusters that do not satisfy the criterion after *max\_it* iterations will be marked as noise. As for the correctness criterion, we configured a threshold on the standard deviation of velocities inside each cluster, so that to define a maximum width of its distribution of velocities.

For the analysis later presented, we calibrated manually the algorithm and we set the parameters as  $(minPoints, \Theta_\nu, max\_it, \Delta_{points}) = (3, 10^\circ, 5, 2)$ . Results highlighted a significant improvement achieved with this extension.

The second step reflects the definition provided in [11]. It works sequentially on individual clusters previously identified, by using a distance metric able to characterize *queueing* pedestrians. This step analyses pedestrians positions and the average velocity  $\vec{V}_{C^*}$  (Eq. 24) of the associated cluster  $C^*$  found with the previous step, if any. The applied distance metric  $\Lambda_{ij}$  aims, in fact, at aggregating points following the direction of movement. With this purpose, the metric defines an elliptical neighbourhood, in which the ellipse is rotated in order to have its long side parallel to the direction of motion described by  $\vec{V}_{C^*}$ . This is formalized in the following equations:

$$\Lambda_{ij} = \sqrt{\left(\frac{\hat{x}_{ij}}{\Xi_x}\right)^2 + (\hat{y}_{ij})^2} \quad (21)$$

$$(\hat{x}_{ij}, \hat{y}_{ij}) = \odot \left( \vec{x}_j - \vec{x}_i, -\angle \left( \vec{V}_{C^*}, (1, 0) \right) \right) \quad (22)$$

$$\angle(\vec{\nu}_i, \vec{\nu}_j) = \begin{cases} \alpha_{ij} & \text{if } DET(\vec{\nu}_i, \vec{\nu}_j) \leq 0 \\ 360 - \alpha_{ij} & \text{otherwise} \end{cases} \quad (23)$$

$$\vec{V}_{C^*} = \sum_{j \in C^*} \left( \frac{\vec{\nu}_j}{|C^*|} \right) \quad (24)$$

Here  $\odot$  rotates counter-clockwise the vector  $\vec{x}_j$  w.r.t  $\vec{x}_i$  by the degrees described with the second input.  $\angle$  computes the clockwise angle between the two input vectors ( $DET$  is the determinant of the matrix built with  $\vec{\nu}_i$  and  $\vec{\nu}_j$ ). Regarding this passage, we configured the parameters as  $(minPoints, \Theta_x, \Xi_x) = (3, 0.8m, 3)$ .

## 5 Results

Figure 2 shows the time evolution of the  $\nu$  observable in the  $\rho = 1$  ped/m<sup>2</sup> condition, while Figure 3 shows the corresponding result in the  $\rho = 4$  ped/m<sup>2</sup> condition. We may observe that the effect of groups on velocity is very strong in the medium density range, in which flows without groups present a clearly higher velocity. The velocity difference is higher than the one between groups and individuals in moderate density settings [4]. On the other hand, the effect of the presence of groups on velocity is not present at very high densities.

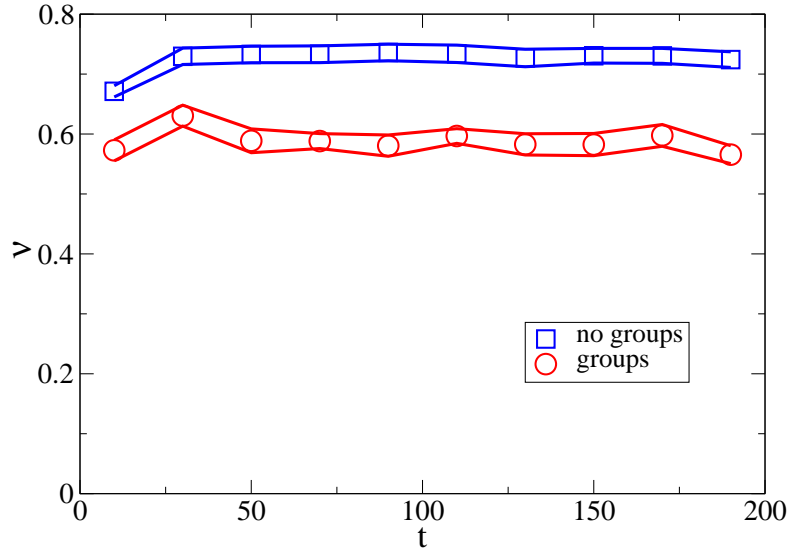


Figure 2:  $\nu(t)$  for the  $\rho = 1$  ped/m<sup>2</sup> condition. Blue and squares correspond to  $r_g = 0$ , while red and circles to  $r_g = 0.5$ . Continuous lines correspond to standard error confidence intervals.

Figure 4 shows the time evolution of the  $E$  observable in the  $\rho = 1$  ped/m<sup>2</sup> condition, while Figure 5 shows the corresponding result in the  $\rho = 4$  ped/m<sup>2</sup> condition. We may observe that the amount of collision is strongly increased in presence of groups for any value of  $\rho$ .

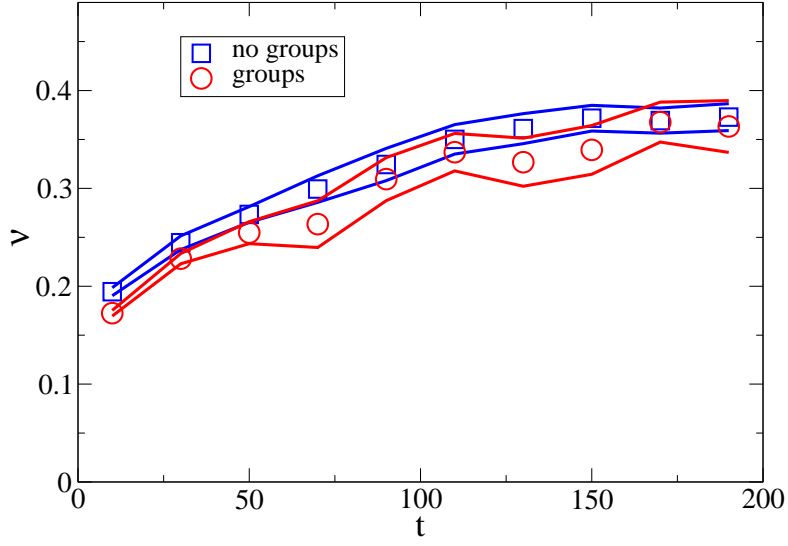


Figure 3:  $\nu(t)$  for the  $\rho = 4$  ped/m<sup>2</sup> condition. Blue and squares correspond to  $r_g = 0$ , while red and circles to  $r_g = 0.5$ . Continuous lines correspond to standard error confidence intervals.

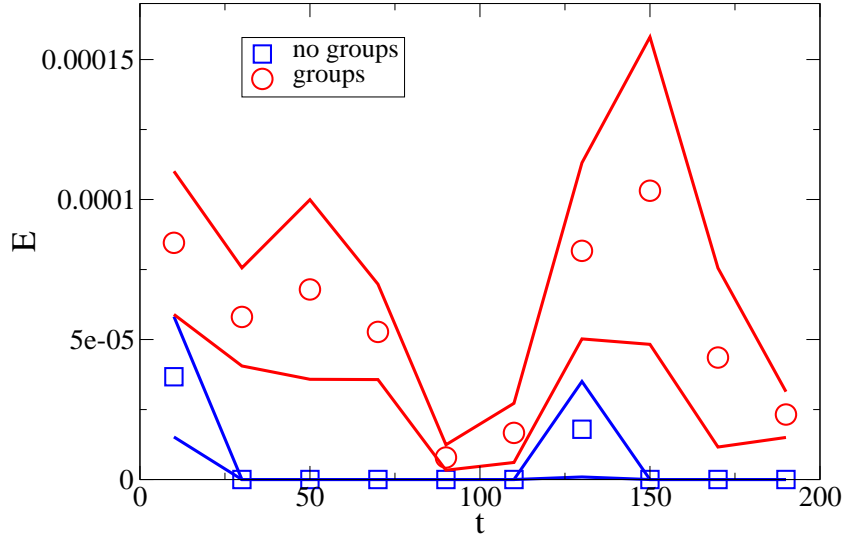


Figure 4:  $E(t)$  for the  $\rho = 1$  ped/m<sup>2</sup> condition. Blue and squares correspond to  $r_g = 0$ , while red and circles to  $r_g = 0.5$ . Continuous lines correspond to standard error confidence intervals.  $E$  is measured as kinetic energy corresponding to a mass 1 exchanged in average by a pedestrian each second.

Figure 6 shows the number of lanes in the  $\rho = 2$  ped/m<sup>2</sup> condition in absence and presence of groups. Although the number of lanes stabilises around 3 in both cases, in the

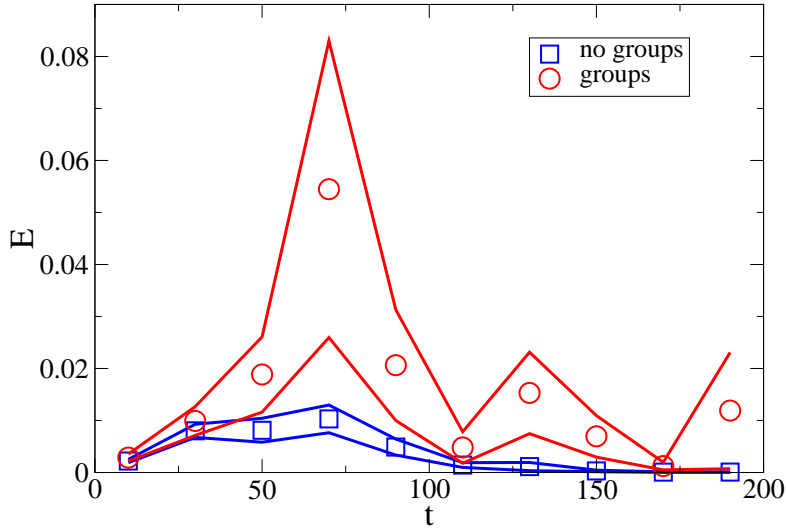


Figure 5:  $E(t)$  for the  $\rho = 4$  ped/m<sup>2</sup> condition. Blue and squares correspond to  $r_g = 0$ , while red and circles to  $r_g = 0.5$ . Continuous lines correspond to standard error confidence intervals.  $E$  is measured as kinetic energy corresponding to a mass 1 exchanged in average by a pedestrian each second.

initial stage the flows with groups present an higher number of lanes. The corresponding result in the  $\rho = 3$  ped/m<sup>2</sup> condition is shown in Figure 7. In this case also the final number of lanes is different, converging to 3 in absence of groups, and 2 in presence of groups (see also figures 8, 9; the presence of groups occupying a wider space makes the formation of three lanes more difficult).

Finally, Figure 10 shows the rate of pedestrians in lanes in the  $\rho = 2$  condition in absence and presence of groups. As it happens in general, a larger number of pedestrians is organised in lanes when groups are absent.

## 6 Conclusions

We have verified that by combining a realistic model for group behaviour at moderate crowd density with an efficient collision avoidance model, the presence of groups has a strong impact on the dynamics of bi-directional flows, affecting the velocity of pedestrians, the amount of collisions between pedestrians, the number of lanes and the rate of pedestrians organised in lanes.

By trying to move on specific formations to enhance not only proximity but also communication between the group members (abreast and V formations) groups occupy a larger portion of the corridor and have less moving flexibility. Their presence decreases the average velocity of the crowd, makes organisation in lanes more difficult and increases the number of collisions.

We have no claim that these results reflect the reality of the effect of groups on crowd

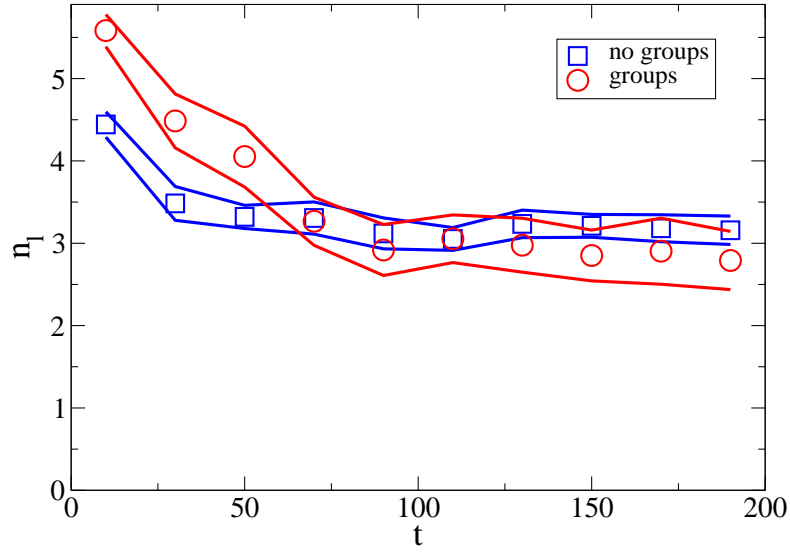


Figure 6:  $n_l(t)$  for the  $\rho = 2$  ped/m<sup>2</sup> condition. Blue and squares correspond to  $r_g = 0$ , while red and circles to  $r_g = 0.5$ . Continuous lines correspond to standard error confidence intervals.

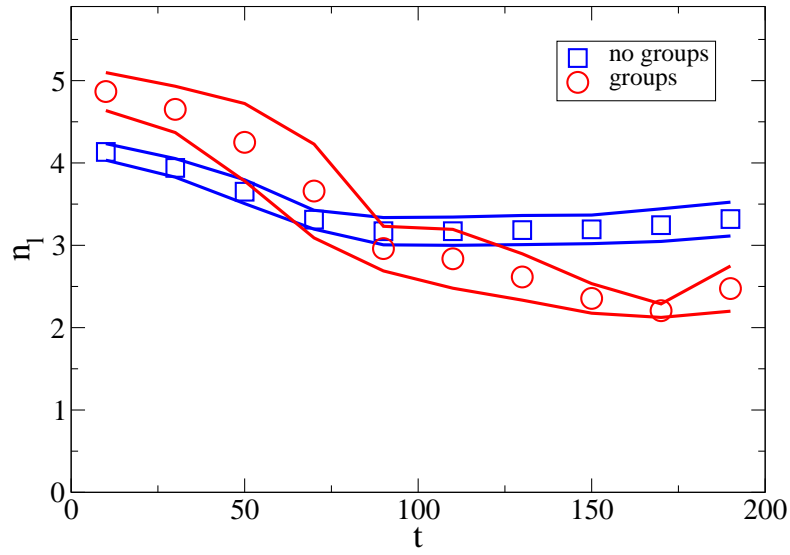


Figure 7:  $n_l(t)$  for the  $\rho = 3$  ped/m<sup>2</sup> condition. Blue and squares correspond to  $r_g = 0$ , while red and circles to  $r_g = 0.5$ . Continuous lines correspond to standard error confidence intervals.

dynamics. Although the impact on velocity and lane organisation goes in the expected direction and seems reasonable at least from a qualitative point of view, it is questionable

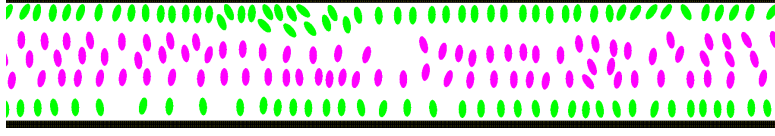


Figure 8: Simulation snapshot for  $\rho = 3 \text{ ped/m}^2$  and  $r_g = 0$ . Green move to the left; violet to the right.

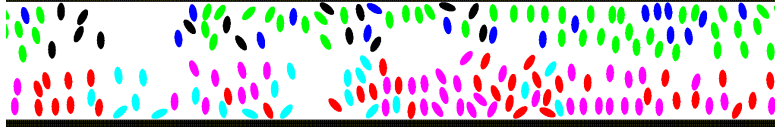


Figure 9: Simulation snapshot for  $\rho = 3 \text{ ped/m}^2$  and  $r_g = 1$ . Green move to the left; red, violet (dyads) and cyan (triads) to the right. Green, black (triads) and blue (dyads) move to the left; violet, red (dyads) and cyan (triads) to the right.

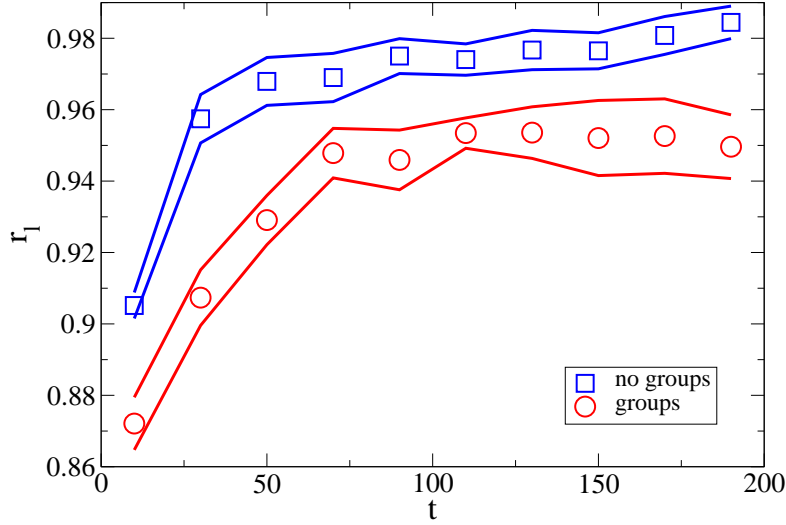


Figure 10:  $r_l(t)$  for the  $\rho = 2 \text{ ped/m}^2$  condition. Blue and squares correspond to  $r_g = 0$ , while red and circles to  $r_g = 0.5$ . Continuous lines correspond to standard error confidence intervals.

that crowds with groups present such a larger amount of collisions. Just combining a collision avoidance and a group behaviour model could overlook important aspects such as a specific behaviour of pedestrians *towards* groups, and a density-dependent tendency of groups to give up communication and thus spatial formations to avoid collisions.

We nevertheless believe that our preliminary results seriously hint at problems and difficulty of a naive approach to the presence of groups in crowds.

## 7 Acknowledgements

This research is partially based on results obtained from a project commissioned by the New Energy and Industrial Technology Development Organization (NEDO).

## References

- [1] Reicher, SD, *The psychology of crowd dynamics*, Vol. 44. No. 0. Blackwell handbook of social psychology: Group processes, 2001.
- [2] M. Schultz, L. Rößger, F. Hartmut and B. Schlag, *Group dynamic behavior and psychometric profiles as substantial driver for pedestrian dynamics*, in *Pedestrian and Evacuation Dynamics 2012*, U. Weidmann, U. Kirsh and M. Schreckenberg, Vol II, pp. 1097-1111 (2014)
- [3] F. Zanlungo, T. Ikeda, T. Kanda, *Potential for the dynamics of pedestrians in a socially interacting group*, Phys. Rev. E, 89, 1, 021811, (2014)
- [4] F. Zanlungo, D. Bršćić and T. Kanda, *Spatial-size scaling of pedestrian groups under growing density conditions* Physical Review E 91 (6), 062810 (2015)
- [5] He L, Pan J, Wang W and Manocha, D, *Proxemic group behaviors using reciprocal multi-agent navigation*, 2016 IEEE International Conference on Robotics and Automation (ICRA), 292–297.
- [6] M. Moussaïd, N. Perozo, S. Garnier, D. Helbing and G. Theraulaz, *The walking behaviour of pedestrian social groups and its impact on crowd dynamics*, PLoS One, 5, 4, e10047, (2010)
- [7] Costa M, *Interpersonal distances in group walking*, Journal of Nonverbal Behavior, 2010, 34, 1, 15-26.
- [8] Zanlungo F, and Kanda T, *Do walking pedestrians stably interact inside a large group? Analysis of group and sub-group spatial structure*, COGSCI13 (2013 Cognitive Science Society Conference).
- [9] Gorrini A, Vizzari G, and Bandini S, *Granulometric distribution and crowds of groups: focusing on dyads*, 11th Conference International Traffic and Granular Flow, Delft (NL), (2015)
- [10] Bandini S, Crociani L, Gorrini A, and Vizzari G, *An agent-based model of pedestrian dynamics considering groups: A real world case study*, IEEE 17th International Conference on Intelligent Transportation Systems (ITSC), 2014, 572–577.
- [11] Crociani L, Vizzari G, Gorrini A, and Bandini S *Identification and Characterization of Lanes in Pedestrian Flows Through a Clustering Approach*. International Conference of the Italian Association for Artificial Intelligence (AIIA), 2018, 71–82.



- [12] Ester M, Kriegel HP, Sander J, and Xu X, *A density-based algorithm for discovering clusters in large spatial databases with noise*, Kdd, Volume 96, No. 34, 1996, 226–231.
- [13] Köster G, Seitz M, Tremel F, Hartmann D, and Klein W, *On modeling the influence of group formation in a crowd*, Contemporary Social Science, 2011, 6, 3, 397-414.
- [14] Köster G, Tremel F, Seitz M, and Klein W, *Validation of crowd models including social groups*, In *Pedestrian and Evacuation Dynamics 2012*, Weidmann U, Kirsh U, and Schreckenberg M editors, Vol II, pp. 1051-1063; Springer; 2014.
- [15] Wei X, Lv X, Song W, and Li X, *Survey study and experimental investigation on the local behavior of pedestrian groups*, Complexity, Volume 20, Issue 6 July/August 2015, pp. 8797.
- [16] Karamouzas I, and Overmars M, *Simulating the local behaviour of small pedestrian groups*, Proceedings of the 2010 17th ACM Symposium on Virtual Reality Software and Technology, 183-190.
- [17] Zhang Y, Pettré J, Qin X, Donikian S, and Peng Q, *A local behavior model for small pedestrian groups*, 12th International Conference on Computer-Aided Design and Computer Graphics (CAD/Graphics), 2011, 275-281.
- [18] Bode N, Holl S, Mehner W, and Seyfried A, *Disentangling the impact of social groups on response times and movement dynamics in evacuations*, PLoS one <http://dx.doi.org/10.1371/journal.pone.0121227>
- [19] Gorrini A, Crociani L, Feliciani C, Zhao P, Nishinari K, and Bandini S, *Social groups and pedestrian crowds: experiment on dyads in a counter flow scenario*, Proceedings of the 2016 Pedestrian and Evacuation Dynamics Conference.
- [20] Zhao P, Sun L, Cui L, Luo W, and Ding Y, *The walking behaviours of pedestrian social group in the corridor of subway station*, Proceedings of the 2016 Pedestrian and Evacuation Dynamics Conference.
- [21] von Krüchten C, Müller F, Svachiy A, Wohak O, and Schadschneider A, *Empirical study of the influence of social groups in evacuation scenarios*, Traffic and Granular Flow '15 (Springer, 2016)
- [22] Wang W, Lo S, Liu S, and Ma J, *A simulation of pedestrian side-by-side walking behaviour and its impact on crowd dynamics*, Proceedings of the 2016 Pedestrian and Evacuation Dynamics Conference.
- [23] Huang J, Zou X, Qu X, Ma J, and Xu R, *A structure analysis method for complex social pedestrian groups with symbol expression and relationship matrix*, Proceedings of the 2016 Pedestrian and Evacuation Dynamics Conference.

- [24] Manfredi M, Vezzani R, Calderara S and Cucchiaro R, *Detection of static groups and crowds gathered in open spaces by texture classification*, Pattern Recognition Letters, 44, 39-48 (2014).
- [25] von Krüchten C, and Schadschneider A, *Empirical study on social groups in pedestrian evacuation dynamics*, Physica A: Statistical Mechanics and its Applications, 475, 129-141, (2017)
- [26] Faria JJ, Dyer JR, Tosh CR and Krause J, *Leadership and social information use in human crowds*, Animal Behaviour, 79(4), 895-901 (2010)
- [27] Templeton A, Drury J and Philippides A, *From mindless masses to small groups: conceptualizing collective behavior in crowd modeling*, Review of General Psychology, 19(3), 215 (2015).
- [28] Zanlungo, F., Yücel, Z., Bršćić, D., Kanda, T, and Hagita, N., *Intrinsic group behaviour: Dependence of pedestrian dyad dynamics on principal social and personal features*, PLoS one, 12, 11, e0187253 (Public Library of Science, 2017)
- [29] Zanlungo, F., Yücel, Z., Kanda, T, and Hagita, N., *Intrinsic group behaviour2:* , PLoS 2019
- [30] Zanlungo F, and Kanda T, *A mesoscopic model for the effect of density on pedestrian group dynamics*, EPL (Europhysics Letters), 2015; 111, 38007.
- [31] Zanlungo, F., Yücel, Z., Ferreri, F., Even, J., Saiki, L. Y. M., & Kanda, T. (2017, November). *Social group motion in robots*. In International Conference on Social Robotics (pp. 474-484). Springer, Cham.
- [32] Zanlungo, F., Ikeda, T., and Kanda, T. (2011). *Social force model with explicit collision prediction*. EPL (Europhysics Letters), 93(6), 68005.
- [33] Helbing, D., and Molnar, P. (1995). *Social force model for pedestrian dynamics*. Physical review E, 51(5), 4282.
- [34] Zanlungo, F. (2007). *Microscopic dynamics of artificial life systems* (Doctoral dissertation, Alma Mater Studiorum).
- [35] Foulaadvand, M. E., and Yarifard M. *Two-dimensional system of hard ellipses: A molecular dynamics study* Physical Review E 88.5 (2013): 052504.